Progress In Electromagnetics Research, PIER 101, 75–96, 2010

NOVEL LOW-COST END-WALL MICROSTRIP-TO-WAVEGUIDE SPLITTER TRANSITION

H. Aliakbarian

Katholieke Universiteit Leuven (KUL)
Leuven, Belgium

A. Enayati †

Interuniversity Microelectronics Centre (IMEC)
Leuven, Belgium

G. A. E. Vandenbosch

Katholieke Universiteit Leuven (KUL)
Leuven, Belgium

W. De Raedt

Interuniversity Microelectronics Centre (IMEC)
Leuven, Belgium

Abstract—A novel configuration for an end-wall microstrip-to-waveguide splitter transition is presented suitable for use in series fed microstrip arrays. The low price, simplicity, manufacturability, low sensitivity, and also wideband operation, up to more than 37%, is the result of positive interaction between double slots and double stubs. The transition is applied to a dual band 1×2 array. A wideband non-tilted pattern is achieved.

1. INTRODUCTION

Although it is highly desirable to select planar structures due to their lower cost and complexity and also their low profile, metal hollow waveguides are still key functional parts in many circuits, especially at millimeter frequencies. These waveguides are usually needed in

Corresponding author: H. Aliakbarian (hadi.aliakbarian@esat.kuleuven.be).
† Also with Katholieke Universiteit Leuven (KUL), Leuven, Belgium.

antenna feeds, high-Q components, duplexers, and low phase noise oscillators. At these higher frequencies, the waveguide bulkiness is no longer an important factor and its losses are smaller than those of a microstrip line. Thus, a well-designed practical transition from a waveguide to a microstrip line becomes an important point.

Several types of transitions from waveguide to microstrip line have been reported in literature, but the most common types of transitions are the probe type transition [1–3], the transition via antipodal finline [4], the transition via a ridged waveguide [5], the quasi-Yagi type [6], and the planar waveguide type [7]. The last three are so-called "longitudinal" transitions. Although some of these types have wideband characteristic, most of them suffer from several disadvantages such as manufacturing complexity and relatively large bulkiness. Also, it is difficult to integrate them with the planar circuits. The goal of this paper is to introduce a new transition topology. The practicality of the new topology will be illustrated by using it in a feeding network for a series fed microstrip array. A few of the transitions mentioned above are useful to feed planar antenna arrays [8, 9]. However, we are looking for a new class of splitter/combiner transitions to overcome the disadvantages mentioned.

The novel configuration consists of an end-wall connection between a simple metal waveguide and a double sided etched substrate, shown in Fig. 1. There is a double slit in the ground of the substrate, coupling the wave to two microstrip ports. Also, two stubs are added to the microstrip line. This novel, easily-manufacturable structure, if designed properly, lowers the cost, size and complexity, and improves

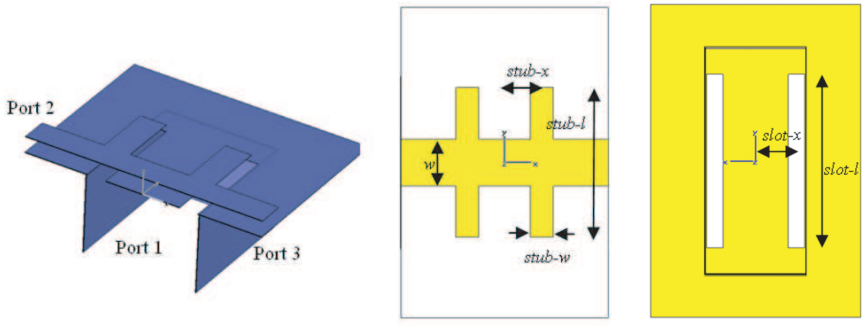

(a) 3D view. (b) Top stub view. (c) Bottom slot view.

Figure 1. The configuration of the double slot microstrip-to-waveguide transition.

the bandwidth of the transition. This transition can be terminated in one port and serve as a single-end transition, or it can be designed as a two-way power splitter/combiner. The structure was introduced in [10]. In [11], we have considered the effects of different substrates on the transition performance at 12 GHz. In this paper, we thoroughly investigate the advantages of the transition over other topologies and show its feasibility at different frequencies. The structure is fabricated and simulation results are compared to practical measurements as also presented in [11].

2. END-WALL TRANSITIONS IN THE LITERATURE

For an optimal design of a transition, the requirements are a minimum return loss at the input of the waveguide, and minimum radiation from the coupling slots. We start with a simple structure which is the end-wall connection between a metal waveguide and a microstrip line with a single slot in the ground depicted in Fig. 2(a). A slot fed microstrip antenna has been used to couple a cavity resonator to a microstrip line by Scheck [12].

Using this idea, many microstrip-to-waveguide transitions have been presented. This kind of transitions, with one slot in the ground, is narrow banded as a result of the high impedance difference between waveguide and microstrip, proportional to the difference between dielectric constant of the substrate and material in the waveguide [8]. The other problem pointed out is back scattering of the transition which is another expression of the mismatch in the waveguide port. Most of the power flowing in the waveguide returns from the end-wall of the guide. Hence, it is hard to achieve a proper impedance match of the waveguide input in this structure.

Obviously, although coupling aperture enlargement increases the coupling level, it decreases the coupling efficiency because of the increase in radiation loss due to the resonant length of the coupling slot. However, if the signal level received in the microstrip ports

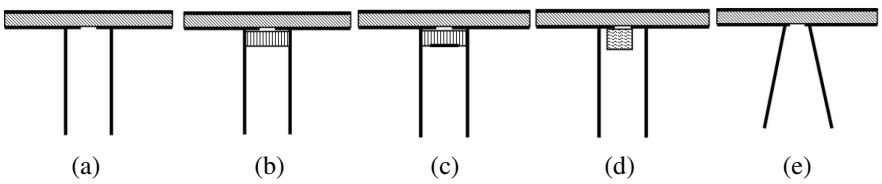

Figure 2. Different configurations for end-wall waveguide to microstrip transition.

is maximized, the radiation loss from the slot will be minimized proportionally as well. Pozar [13] pointed out that the end-wall connection of the guide causes strong reflection which prevents us from matching the waveguide input in Fig. 2(a), even for a good coupling. Of course, if a coupling of more than −3.4 dB is reached the reflection automatically will be reduced. Also, a microstrip-line fed resonant slot has very high series impedance. To reduce this impedance one can offset the feed line from the centre of the slot or use matching transformers as in [14]. However, about half of the input power will be radiated at the microstrip side of the structure [13]. Moreover, offsetting the slot from the center increases the cross polarization if used inside an antenna.

Very recently, a successful narrow band design, similar to Fig. 2(a), using only one slot in the ground has been reported at 140 GHz [15]. However, the simulated −10 dB return loss and 1 dB insertion loss bandwidth are about 2% which is too small for most applications. Having said that, this transition design is highly dependent on the frequency, relative thickness of the substrate, and its dielectric constant, meaning that designs for other specific situations, possibly at different frequencies and with different substrates, have not been reported. In this paper a similar structure is designed and compared to the new structure in Section 4.

Villegas and Stones have modified the mentioned structure using a bulky metal cavity enclosure and a broadband matching stub. Then, using a broadband microstrip end at one side, a bandwidth of 10% is achieved. Clearly, the closed bulky structure can not be used for array feeding [8].

Using a piece of dielectric in the waveguide part, as shown in Fig. 2(b), acting as a matching transformer, yields an improved return loss [8, 13, 16]. This method eliminates the need for a specially formed waveguide junction. It is of course true that the practical implementation is much more difficult and more expensive than that of Fig. 2(a).

In Fig. 2(c), a patch is added to the additional substrate to improve the bandwidth. This transition is similar to that of Grabherr [16], whose topology was modified by Hyvonen [8]. The main difference between the two is the position of the dielectric. Hyvonen put it close to the aperture above the patch, while Grabherr is putting it below the patch. The former needs a high precision waveguide step to place the dielectric, which is more complicated for manufacturing. Another similar configuration has been employed by Wang [17] in a multi-layered LTCC. In Grabherr's work, a bandwidth of more than 10% for a −15 dB return loss and a 0.3 dB transition loss has been

claimed, while Hyvonen reported 16% of −20 dB bandwidth. Wang achieved 8.5% for S_{11} less than −15 dB for a single ended transition. It is observed in the Hyvonen measurements that the use of a dielectric part in the waveguide, as in Fig. 2(b) or Fig. 2(c), apparently causes extra resonances [13]. Unfortunately, none of the resonances are predicted, neither using Ansoft HFSS nor CST Microwave studio [18]. In fact, in our view, a thin dielectric piece with an effective height of one third of a wavelength cannot cause multiple resonances. In all of the modified solutions described above, it has not been taken into consideration that substrates only exist in a limited range of thicknesses and dielectric constants. A successful design for a specific problem is thus no guarantee that this is also possible for other problems.

In the discussed improved version of the end-wall transition, the microstrip patch acts like an 'antenna' that transmits energy from the waveguide to the slot, and vice versa. Leung and So [19] use a dielectric resonator instead of a microstrip patch, as shown in Fig. 2(d). In the new configuration, the DR also acts as an antenna. However, the design is even more narrowband, with a −10 dB bandwidth of 2.4%, albeit for a simple design and implementation.

The most wideband design of an end-wall transmission has been proposed by Davidovitz [9], a tapered transition, depicted in Fig. 2(e). The key idea in this transition is the tapered section of the waveguide feeding the aperture in the microstrip ground. This taper matches the high impedance of the standard guide and the relatively low impedance of the reduced-height waveguide. Thus the problem of the high series impedance in the microstrip is solved and operation in the whole waveguide band is provided. In splitter/combiner configurations, each microstrip port receives −3.7 dB of power in a full wave simulation that we performed for this structure. Disadvantages are that the transition needs an expensive high precision fabrication and also its length is large. To be more specific, the transition of [9] has a 15.2 cm tapering length in the X-band. Including additional transition pieces, the total length is more than 20 cm, which is more than six wavelengths. Simulation shows that the performance is acceptable for smaller tapering lengths.

To block radiation from the waveguide apertures and to guide power into the microstrip ports, a good suggestion is to use a non-resonant plate on top of the waveguide and substrate. We have investigated this idea and the configuration was not successful without some complementary modifications. Choi and Lee [20] used the plate in addition to a dog-bone shape iris placed below a piece of formed waveguide, as shown in Fig. 3(a), to feed a one by two array antenna.

Although the technique removes the need for special dielectrics, it still requires costly waveguide shaping. It has been stated in [20] that the role of the iris, placed 0.4 wavelengths from the plate, is to create a resonance within the working frequency band. The modifications match the transition, but the amount of radiation generated by the plate is still an open question. Note that the radiation is co-polarized with the radiation of the patches. In our view, an important design parameter is the distance between the slot and the plate, which allows optimizing the matching of the high impedance resonant slot to the microstrip line. On the 0.7874 mm (31 mil) Taconic TLX-9 substrate, the bandwidth reached is no more than 9%, even with the use of the dog-bone slot [21].

Another coupling topology using a covering plate is shown in Fig. 3(b). It uses so-called proximity coupling, introduced by Iizuka et al. [22, 23]. It is similar to our work because of the fact that the topology contains a single dielectric substrate attached to the waveguide. Although it needs several metallic vias, it is suitable for mass production. Note that it has in-phase output ports instead of an 180° phase shift. In Iizuka's topology two microstrip lines and a waveguide short with two notches are etched on the top side of the dielectric substrate. The rectangular patch and ground are etched on the backside. Via-holes are placed along the circumference of the waveguide short to connect it electrically to the ground. Thus, the TE_{01} mode coming from the waveguide is converted into the quasi-TEM mode of the microstrip lines, using the dominant mode of the patch element. The final result shows a bandwidth of 6% for a return loss better than −14 dB, limited by the resonances. Thus, the wideband behaviour is governed by the resonance of the patch element in the waveguide.

Another type of end-wall transition introduced in [24] is also

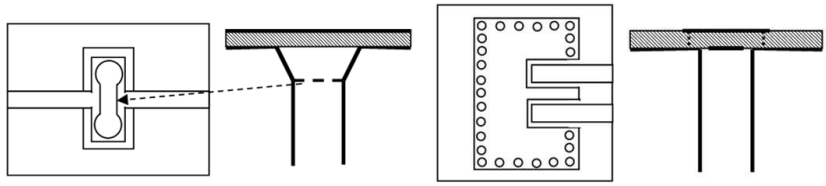

(a) From Choi [19] (top and cross view).

(b) From Iizuka [20] (top and cross view).

Figure 3. End-wall transitions with a blocking plate on top.

wideband and inexpensive. It uses a CPS probe to absorb the wave inside the waveguide and transfer it to microstrip line. The disadvantage is the difficulties of the structure to be integrated in planar circuits and antennas. It also doesn't produce intrinsically out of phase outputs if designed as a splitter.

3. PROPOSED CONFIGURATION

The end-wall configuration proposed in Fig. 1 is useful for modular connections of waveguide components to planar circuits and antennas, and can be inexpensively manufactured since there is no need for specially machined waveguides or for inserting additional parts in the waveguide. Using a well designed end-wall waveguide-to-microstrip transition, it is possible to obtain high levels of coupling, while the structure symmetry guarantees equal power splitting in the two microstrip ports, and a 180-degree difference in their phase. This will generate a non-tilted sharp beam in the planar antenna given later as an application example.

Similar to most of the end-wall splitter transitions, the working principle of this splitter is similar to the one of a waveguide Tee junction. The dominant TE_{01} mode moves into the junction with uniform distribution along x direction as shown in Fig. 4(a). Hence, the fields at the slot points S_1 and S_2 in Fig. 4(b) are the same. The stubs placed on top of the slots block the radiation and can be optimized with respect to coupling and matching. The waves in the microstrip lines can travel in the positive and negative x direction. In total there are four waves like that, named W_1^-, traveling to the left microstrip port, W_2^+, traveling to the right microstrip port, and W_1^+ and W_2^-, traveling in the middle region. Due to symmetry, the last two are out of phase and propagate identically to the point 'C_0'. Obviously, they

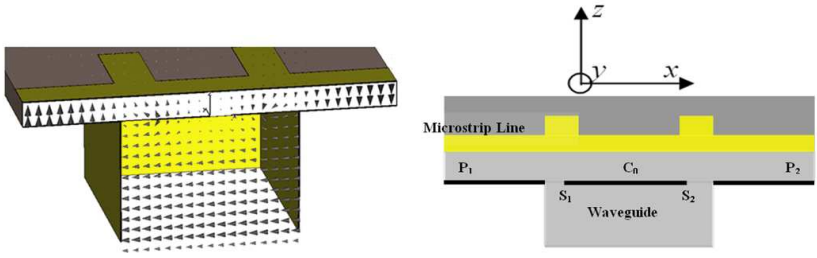

(a): E-field distribution.

(b) Front view of the waveguide junction.

Figure 4. Transition scheme and E-field distribution.

cancel each other and there is no E-field at the center $x = 0$. That is why a blocking centered plate does not work in this configuration. The presence of double slots helps the coupling to be more wideband.

The simplicity of the topology is a big advantage in high frequency bands, where dielectric losses affect the efficiency significantly. It is also worth mentioning that for the example given in this paper, the feeding of a planar antenna array, the simplicity and related low cost of the transition are more important than a 1 or 2 dB reduction in coupling magnitude. In fact, an appropriate design may result in a constructive interference of the power radiated by the transition and the antenna radiation.

The parts in the waveguide along with the slot play the role of an antenna [19]. This antenna radiates the waves coming from the microstrip lines into the waveguide space. In the new structure, a two element array distanced about half a wavelength plays this role.

4. DESIGN OF THE SPLITTER

Essential in a design is the choice of the design tool to be used. Rao et al. [25] set up a well-defined design procedure for the simple configuration of a slot in the end-wall coupling. Unfortunately, their formulation cannot be extended to our structure. In 1985, Pozar initiated aperture coupling in microstrip antennas [26]. More suitable formulations for aperture coupling have been developed since then. However, in the design community the last decade the trend is not to use special design tools any more, but to use full wave analysis tools, as for example in [27], where a MoM technique is used.

Because of the large number of parameters and the fairly sensitive nature of the coupling mechanism for this coupler, the design procedure requires a well established analysis tool. In this work, CST Microwave Studio 2008, a widely known accurate software tool employing the Finite Integration Technique, is used [18].

4.1. Design at 18 GHz

The goal is to design a splitter with a bandwidth of more than 10%, a return loss better than -10 dB, and a transmission coupling to the microstrip ports as flat as possible over the working band. The design involves the connection of the waveguide WR51 to the substrate layers. RT5880 ($t = 0.7874$ mm, $\varepsilon_r = 2.2$), RO4003C ($t = 0.508$ mm, $\varepsilon_r = 3.38$ or 3.55 [27]), and RT6010 ($t = 1.27$ mm, $\varepsilon_r = 10.2$) in the K and K_u band between 16 and 20 GHz are considered.

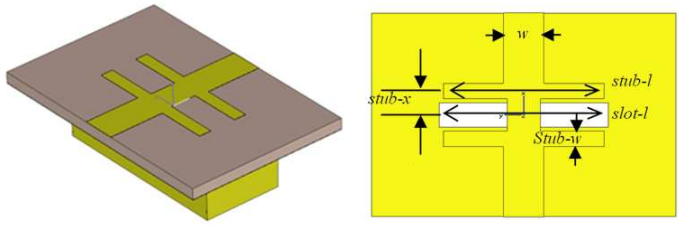

(a) 3D view (b) Top view

Figure 5. Double stub single slot transition configuration.

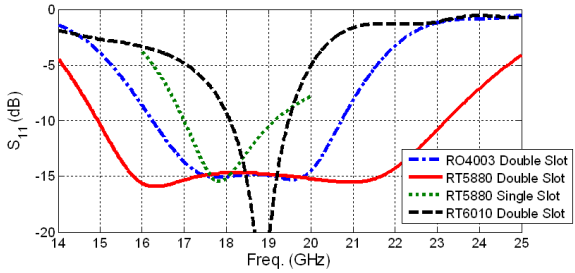

Figure 6. Return loss of the optimized designs.

First we tried to design a power splitter using a single slot in the ground, using RT5880. This failed due to a lack of coupling and a poor return loss. This result is predictable as mentioned in [13]. As discussed in Section 1, it is necessary to match the high impedance waveguide port to the low impedance microstrip line. We tried to transfer the matching problem from the waveguide part to the microstrip part by using double stubs as depicted in Fig. 5. This double stub configuration can be found in the literature [8]. The two matching stubs do help matching the microstrip line to the waveguide. The best case occurs when the two stubs are very close to the slot, without overlapping. An optimization could not reach levels of coupling better than −4.5 dB while having good matching. Return loss and coupling for the best design are shown in Figs. 6 and 7, respectively. Tolerable return loss, better than −10 dB, is seen between 17 and 19 GHz. A coupling of more than −5 dB is observed between 17.3 and 20.8 GHz. Obviously, the 2 dB insertion loss, mostly due to radiation, is not really satisfactory.

The next step was to use double slots and double matching stubs in the microstrip circuit. The idea of using blocking plates above the slots is in some way realized if the stubs are put above the slots. During

the optimization process, we observed that the slots went further and further away from each other, and indeed both stubs were placed on top of the slots automatically, as expected. Fig. 6 and Fig. 7 show the return loss and coupling of the final topologies. Excellent results are achieved on RT5880. The group delays for all four designs are presented in Fig. 8. The two wideband designs on RO4003 and RT5880 have a low deviation within the working band and even outside this band. For the other designs, larger deviations are observed.

The figures illustrate that the bandwidth of the transition is relatively high compared to older types and also highly dependent on the substrate used. The bandwidths are 31.5%, 15% and 4.5% for a -4 dB coupling. The S_{11} bandwidths are somewhat broader. Based on the results, we can conclude that the lower the dielectric constant of the substrate is, the wider the bandwidth that can be expected. All dimensions of the final topologies are given in Table 1 for the three different substrates. It can be seen that the slot lengths are quite longer than half effective wavelength of lowest working frequency and also pretty longer that the stub lengths. All dimensions of the four mentioned designs are indicated in Table 1.

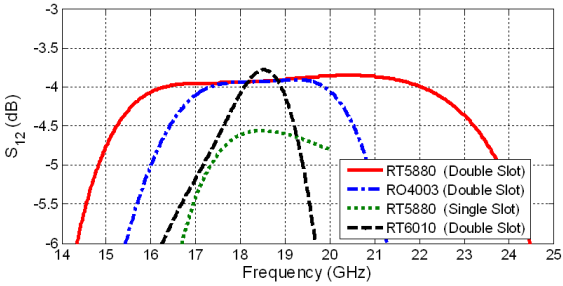

Figure 7. Coupling to microstrip ports for the optimized designs.

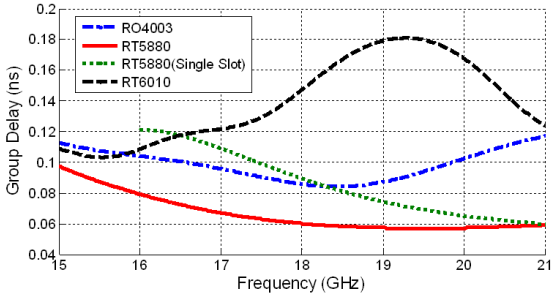

Figure 8. Group delay of the optimized designs.

Table 1. Dimensions of the transitions on RO4003-RT5880-RT6010. Waveguide WR51: 12.95 mm × 5.7 mm.

Variable (in mm)	RO4003	RT5880	RT6010	RT5880 Single slot
Slot-l	10	10	6.5	10
Slot-w	0.79	0.93	1.42	1.43
Slot-x	1.95	2.33	1.33	0.7
Stub-l	8.66	8.66	3.69	9.5
Stub-w	1.7	1.32	3.2	0.91
Stub-x	2.6	2.16	2.2	1.4
W	2.71	2.71	2.61	2.37

4.2. Design at 60 GHz

In order to demonstrate that the transition can be applied at millimeter wave frequencies, the design procedure is repeated on RT5880 ($t = 0.254$ mm $\varepsilon_r = 2.2$) at 60 GHz (V-band) with a WR15 waveguide. Normally, the required 10% bandwidth is difficult to achieve. The design in this section shows a bandwidth of more than 37.7% (57 GHz to 82.7 GHz) for a coupling higher than −4 dB, with good matching at the waveguide port. Compared to the 18 GHz design (bandwidth of 32.2%) a slightly higher bandwidth has been achieved (Fig. 9). At the same time, the return loss is acceptable in the mentioned frequency band (Fig. 10).

It is seen that the dimensions of the both designs have the relation of 68 to 18 approximately, the same as previous designs.

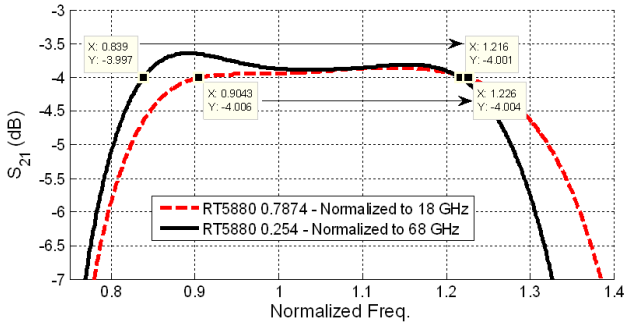

Figure 9. Comparison between S_{21} results for 18 and 60 GHz designs, normalized to the center frequency.

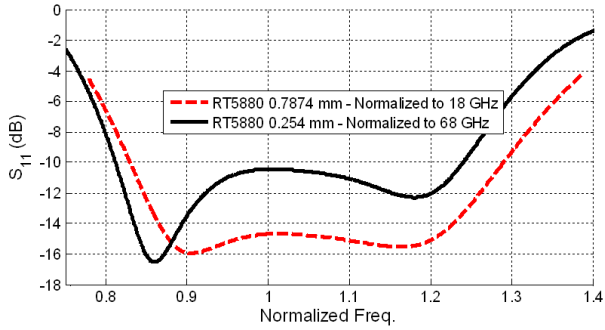

Figure 10. Comparison between S_{11} results for 18 and 60 GHz designs, normalized to the center frequency.

Table 2. Dimensions of the transitions. Waveguide WR15: 3.75 mm × 1.88 mm. Waveguide WR51: 12.95 mm × 5.7 mm.

Variable (in mm)	60 GHz	18 GHz
Slot-l	2.74	10
Slot-w	0.229	0.93
Slot-x	0.62	2.33
Stub-l	1.215	4.33
Stub-w	0.524	1.32
Stub-x	0.58	1.38
W	0.9	2.71

4.3. Practical Design at 12 GHz

To investigate the effect of substrates on the performance of the transition, three different structures have been designed and one has been realized in practice, at 12 GHz, using 3 different substrates, RT5880 ($t = 1.524$ mm, $\varepsilon_r = 2.2$), RO4003 ($t = 0.813$ mm, $\varepsilon_r = 3.38$), and RO4003 ($t = 0.813$ mm, $\varepsilon_r = 3.38$). The double layered substrates are connected to a WR90 waveguide. An X band WR90 waveguide works between 8.2 and 12.4 GHz (standard working range) with a bandwidth of 40%. Thus, the bandwidth of the transition is also limited by the bandwidth of the waveguide.

The results for all three designs are given in Fig. 11 for S_{11} (return loss) and S_{12} (coupling). In fact, the transition can be designed so that it reaches levels of coupling better than −4 dB, but without

wideband operation. We chose to keep the wideband operation. The design on RO-4003 with 0.813 mm thickness is wideband but the coupling level does not get better than −4.5 dB. Using RO-4003 with 1.524 mm thickness, the coupling easily is improved to −4 dB with a flat performance within the 26% bandwidth. The corresponding return loss for these designs in Fig. 11(b) demonstrates that the thicker substrate is matched better as it was expected and stated in Section 1.

Table 3. Dimensions of the transitions. Waveguide WR90: 22.86 mm × 10.16 mm.

Variable (in mm)	**RT5880 1.524 mm**	**RO4003 1.524 mm**	**RO4003 0.813 mm**
Slot-l	16.84	16.8	19
Slot-w	1.37	1.5	1.7
Slot-x	3.76	3.63	3.73
Stub-l	7.4	7.64	7.4
Stub-w	1.77	1.75	3.14
Stub-x	3.45	4.04	6.28
W	4.69	5	4.76

In Fig. 11(a), solid line and dash-point line are coupling for 1.524 mm and 0.813 mm respectively on R0 4003 and RT 5880 substrates. The bandwidth for a coupling of more than −4 dB is about 26% and 35%, respectively, which is excellent for this category of splitter. It shows that the design for a lower permittivity is more wideband. The return loss of the transition within the band is always better than −10 dB.

Figure 11(c) illustrates the group delay for the three designs. Within the working band, the deviation of the group delays is acceptable for all three, but the design on RT5880 1.524 mm is clearly the best.

Photos of the fabricated structure are given in Fig. 12. The measurement results in Fig. 11(a) agree very well with the simulations, although showing some oscillation. The oscillations are more pronounced in Fig. 11(b). The oscillations are mainly due to coaxial to waveguide transition, connection of the thick microstrip lines to the connector, and also soldering of the connector.

Using higher frequencies, like millimeter waves, in some way resembles using thicker substrates. Consequently, as the coupling and return loss of the thicker substrates are superior, it can be understood that the design procedure is much easier in this band.

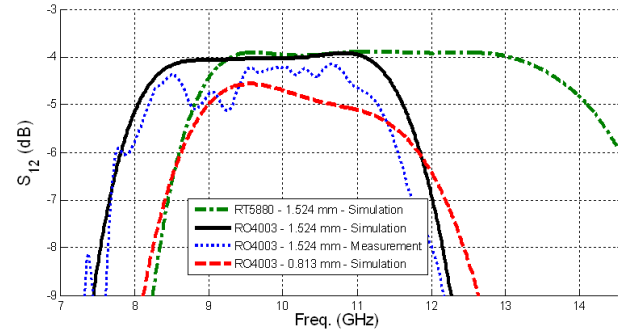

(a) Coupling parameter.

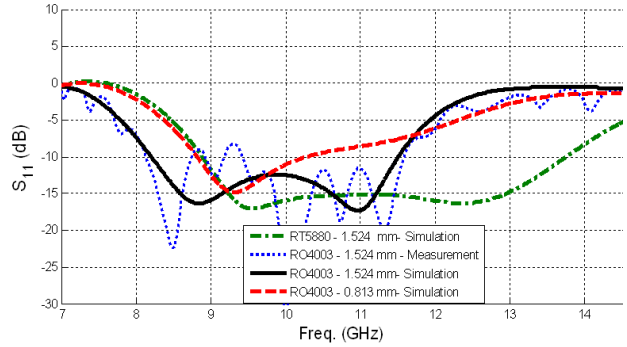

(b) Return loss parameter.

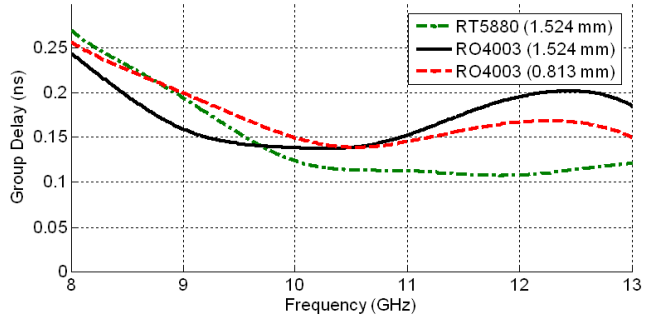

(c) Group delay.

Figure 11. Simulation and measurement results for the 3 designed transitions.

The analysis of the sensitivity of the X-band transition to practical fabrication errors is an important issue that is rarely considered [23]. Fig. 13 to Fig. 17 present the effect of an x translation of the substrate with respect to the waveguide during the fabrication process. The sensitivity of S_{11} and S_{12} should not be too significant. Fig. 13 shows

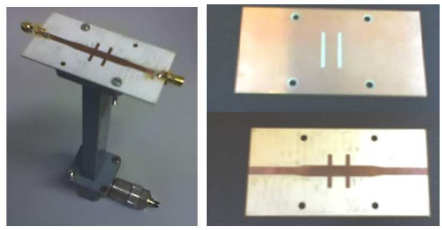

Figure 12. Transition built on RO 4003 1.524 mm.

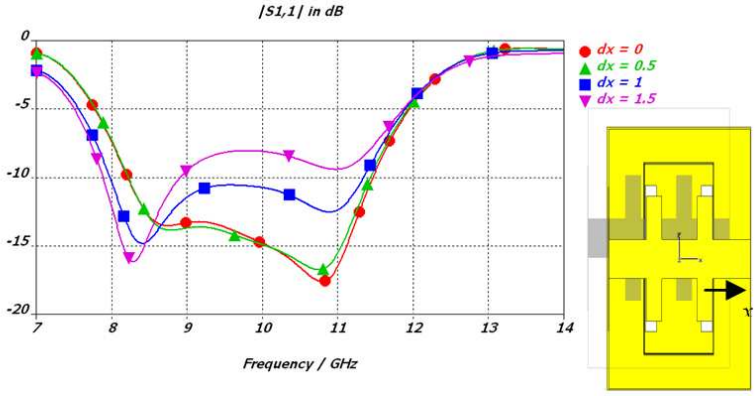

Figure 13. Sensitivity of S_{11} to a translation in x direction, dx in mm.

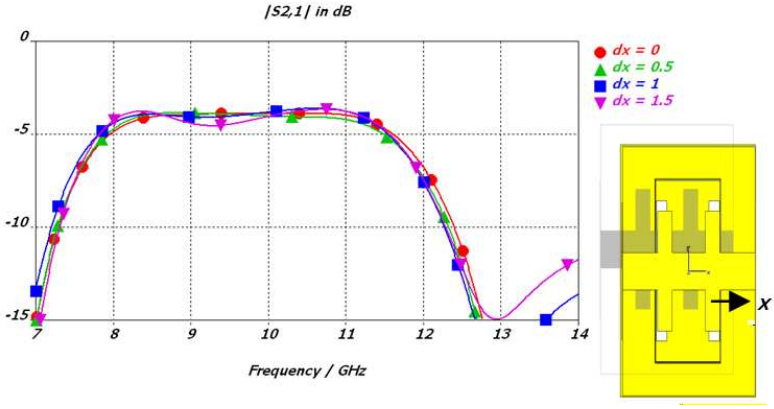

Figure 14. Sensitivity of S_{12} to a translation in x direction, dx in mm.

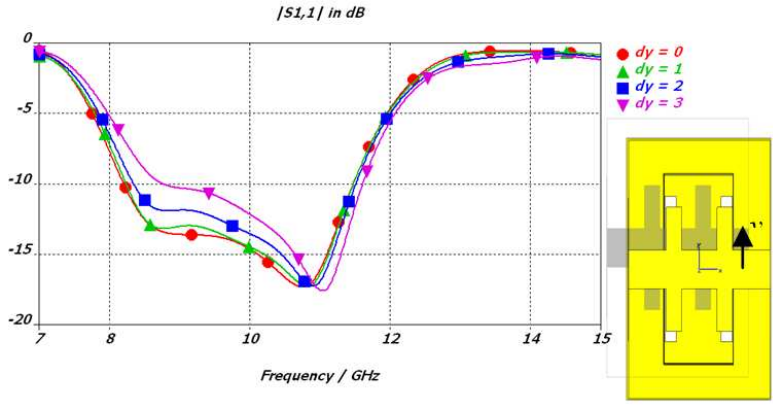

Figure 15. Sensitivity of S_{11} to a translation in y direction, dy in mm.

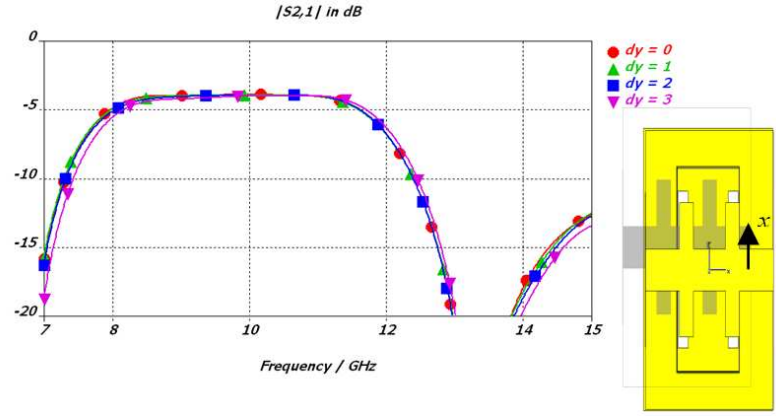

Figure 16. Sensitivity of S_{12} to a translation in y direction, dy in mm.

that a shift up to 1.5 mm in x direction does not really worsen the return loss above the level of -10 dB. Fig. 14 says that the coupling will be kept at the -4 dB level up to this shift. A shift in y direction has less effect on S_{11} at least up to 3 mm, as shown in Fig. 15. Also, a 1.6 mm shift does not cause a real decrease in S_{21} as shown in Fig. 16.

Another important factor to be taken into account is the effect of shifts in the x direction on the symmetry of the structure and thus on the 180 degrees phase difference between the microstrip ports. Fig. 17 shows that a shift of more than 1.5 mm causes a phase unbalance

of more than 40 degrees above 12 GHz. The phase is clearly more sensitive to a translation. The results of this sensitivity analysis, using considerable shifts, illustrate the robustness of the designs.

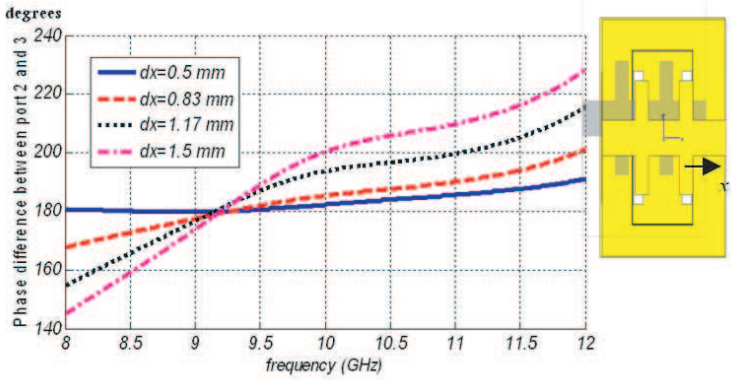

Figure 17. Sensitivity of phase of S_{12} to a translation in x direction.

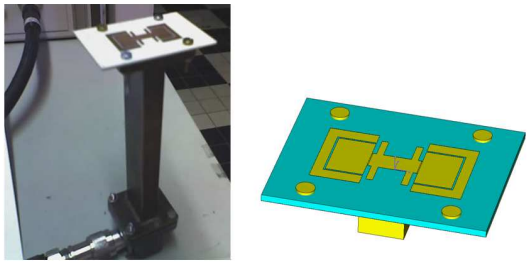

Figure 18. 1×2 array based on the new transition topology.

5. ANTENNA EXAMPLE

As an example of the practical use of the new transition topology, a 1×2 array antenna is considered. The structure is shown in Fig. 18. The transition is based on the substrate RO4003C ($t = 0.813$ mm, $\varepsilon_r = 3.38$). The antenna element is a dual band structure. This allows us to show the non-tilted pattern at the beginning and end of the band, 9 and 10.5 GHz respectively. Each element consists of a square patch and a complementary half ring which is responsible for the second band resonance. The elements are placed near the matching stubs of the transition.

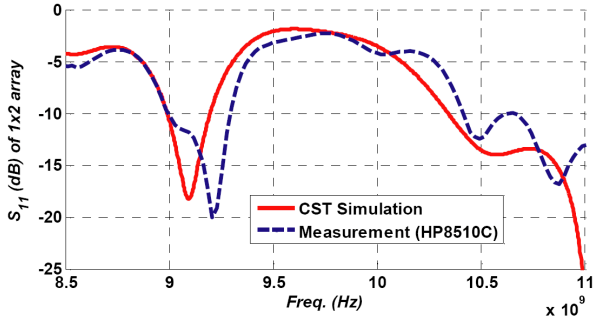

Figure 19. Return loss for the fabricated 1×2 array.

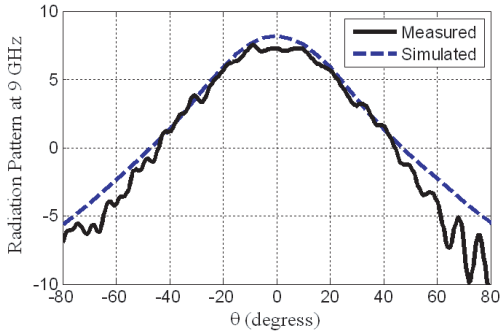

Figure 20. Radiation pattern results of the splitter used for array feeding at 9 GHz.

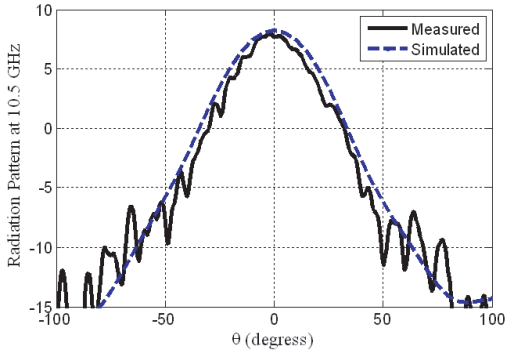

Figure 21. Radiation pattern results of the splitter used for array feeding at 10.5 GHz.

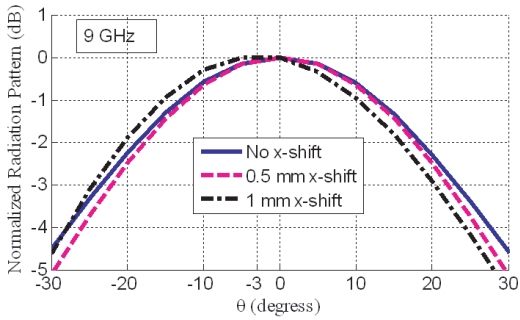

Figure 22. Sensitivity of the radiation pattern to a shift in x direction, 9 GHz.

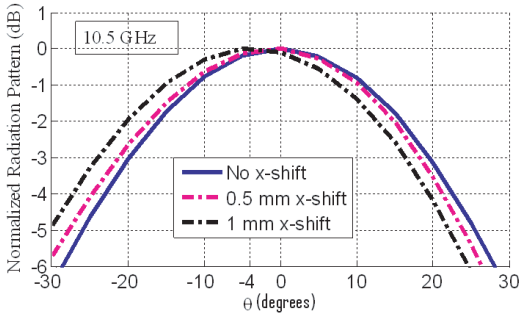

Figure 23. Sensitivity of the radiation pattern to a shift in x direction, 10.5 GHz.

The return loss measurement result, given in Fig. 19, agrees very well with the simulation. Only a negligible frequency shift is observed. More important for this structure is that the main radiation pattern lobe does not change from broad side. The simulation results from CST microwave studio along with measurement results confirm the non-tilted beam at broadside direction at 9 GHz and 10.5 GHz, respectively, which validates the desired out of phased characteristic of the transition for the whole working band. Fig. 20 shows the radiation pattern at 9 GHz and Fig. 21 shows the pattern at 10.5 GHz for φ equal to 0 (E-plane). Another important factor which should be taken into consideration is the sensitivity of the radiation pattern and the direction of the main beam to the mechanical misalignments in antenna manufacturing. This also has been investigated by shifting the antenna with a 0.5 mm and 1 mm respectively in the x direction. The results show that there is no tilt in the radiation pattern for 0.5 mm

shift. However, misalignments more than approximately 1 mm make the radiation pattern starts rotating. The direction of the beam for 1 mm shift is 3° and 4° for 9 GHz and 10.5 GHz respectively. The reason of this tilt is that the edge of the slot has 0.7 mm distance from the edge of the connected waveguide. Thus, increasing the shift from 0.7 mm causes an unbalance in the symmetrical feeding of the lines which itself causes the beam to tilt.

6. CONCLUSION

A new kind of waveguide to microstrip transition has been introduced and verified. Different double slit transitions designed for the 12, 18 and 60 GHz bands have shown that the new topology can be designed wideband. As an example of practical use, one of the designs is applied to a dual band 1×2 array in X-band. The simulation and measurement results confirm the wideband functioning of the transition and the non-rotated pattern in both bands.

REFERENCES

1. Ho, T. Q. and Y. Shih, "Spectral-domain analysis of E-plane waveguide to microstrip transitions," *IEEE Trans. Microwave Theory Tech.*, Vol. 37, No. 2, 388–392, Feb. 1989.
2. Leong, Y. and S. Weinreb, "Full band waveguide to microstrip probe transitions," *IEEE MTT-S Int. Microw. Symp. Dig.*, Vol. 4, 1435–1438, May 1999.
3. Tikhov, Y., J. W. Moon, Y. J. Kim, and Y. Sinelnikov, "Refined characterization of E-plane waveguide to microstrip transition for millimeter-wave applications," *2000 Asia-Pacific Microwave Conference*, 1187–1190, Dec. 2000.
4. Lavedan, L. J., "Design of waveguide-to-microstrip transition specially suited to millimetrewave applications," *Electronic Letters*, Vol. 13, No. 20, 604–605, Sept. 1977.
5. Moochalla, S. S. and C. An, "Ridge waveguide used in microstrip transition," *Microwaves and RF*, Vol. 23, 149–152, Mar. 1984.
6. Kaneda, N., Y. Qian, and T. Itoh, "A broadband microstrip-to-waveguide transition using quasi-Yagi antenna," *IEEE Trans. Microwave. Theory Tech.*, Vol. 47, No. 12, 2562–2567, Dec. 1999.
7. Deslandes, D. and K. Wu, "Integrated microstrip and rectangular waveguide in planar form," *IEEE Microw. Wireless Compon. Lett.*, Vol. 11, No. 2, 68–70, Feb. 2001.

8. Hyvonen, L. and A. Hujanen, "A compact MMIC-compatible microstrip to waveguide transition," *IEEE MTT-S Int. Microw. Symp. Dig.*, Vol. 2, 875–878, Jun. 1996.
9. Davidovitz, M., "Wide band waveguide to microstrip transition and power splitter," *IEEE Microw. Guided Wave Lett.*, Vol. 6, No. 1, 13–15, Jan. 1996.
10. Aliakbarian, H., et al., "Low-radiation-loss waveguide-to-microstrip transition using a double slit configuration for microstrip array feeding microwave," *2007 Asia-Pacific Microwave Conference*, 1–4, Bangkok, Thailand, Dec. 2007.
11. Aliakbarian, H., A. Enayati, W. de Raedt, and G. A. E. Vandenbosch, "Substrate effect on X-band design of end-wall double slit microstrip-to-waveguide splitter," presented at EuCAP, Berlin, Germany, Mar. 2009.
12. Scheck, H. O., "A novel method of cavity resonator coupling to microstrip lines," *Proc. of the 21st European Microwave Conference*, 807–809, Stuttgart, Germany, Sept. 1991.
13. Pozar, D. M., "Aperture coupled waveguide feeds for microstrip antennas and microstrip couplers," *Antennas and Propagation Society International Symposium*, Vol. 1, 700–703, 1996.
14. Villegas, F. J. and D. I. Stones, "A novel waveguide-to-microstrip tranistion for millimeter-wave module applications," *IEEE Trans. Microwave Theory Tech.*, Vol. 47, No. 1, Jan. 1999.
15. Herrero, P. and J. Schoebel, "A WR-6 rectangular waveguide to microstrip transition and patch antenna at 140 GHz using low-cost solutions," *2008 IEEE Radio and Wireless Symposium*, 355–358, Jan. 22–24, 2008.
16. Grabherr, W. and W. Menzel, "A new transition from microstrip line to rectangular waveguide," *Proc. of the 22nd European Microwave Conference*, 1170–1175, Espoo, Finland, 1992.
17. Wang, Z., L. Xia, B. Yaii, R. Xu, and Y. Gou, "A novel waveguide to microstrip transition in millimeter-wave LTCC module," *International Symposium on Microwave, Antenna, Propagation and EMC Technologies for Wireless Communications*, 340–343, Hangzhou, China, Aug. 16–17, 2007.
18. CST Microwave Studio 2008, www.cst.com.
19. Leung, K. W. and K. K. So, "Simple and efficient microstrip-to-waveguide transition," *Electronics Letters*, Vol. 38, No. 6, 280–281, Mar. 2002.
20. Choi, S. H. and J. Y. Lee, "Design of 2-array microstrip patch antenna excited by waveguide endwall coupler," *Proceedings of*

Asia-Pacific Microwave Conference, Vol. 4, 4, Suzhou, China, Dec. 2005.

21. Rathi, V., G. Kumar, and P. Ray, "Improved coupling for microstrip aperture coupled antenna," *IEEE Trans. Antenna Propag.*, Vol. 44, No. 8, Aug. 1996.
22. Iizuka, H., T. Watanabe, K. Sato, and K. Nishikawa, "Millimeter-wave microstrip line to waveguide transition fabricated on a single layer dielectric substrate," *IEICE Trans. Commun.*, Vol. 85, No. 6, 1169–1177, Jun. 2002.
23. Iizuka, H., K. Sakakibara, and N. Kikuma, "Millimeter-wave transition from waveguide to two microstrip lines using rectangular patch element," *IEEE Trans. Microwave Theory Tech.*, Vol. 55, No. 5, 899–905, May 2007.
24. Lin, T. H. and R. B. Wu, "A broadband microstrip-to-waveguide transition with tapered CPS probe," *32nd European Microwave Conference*, 617–620, Milan, Italy, Sept. 23–27, 2002.
25. Rao, J. S., K. K. Joshi, and B. N. Das, "Analysis of small aperture coupling between rectangular waveguide and microstrip line," *IEEE Trans. Microwave Theory Tech.*, Vol. 29, 150–154, 1981.
26. Pozar, D. M., "Microstrip antenna aperture-coupled to a microstripline," *Electronics Letters*, Vol. 21, No. 2, 49–50, Jan. 1985.
27. Ho, M. H., M. A. Krzysztof, and K. Chang, "Waveguide excited microstrip patch antenna-theory and experiment," *IEEE Trans. Antenna Propag.*, Vol. 42, No. 8, 1114–1125, Aug. 1994.
28. Janezic, M. D., "High-frequency measurements of dielectric substrate materials," Technical Note 1520, NIST, Gaithersburg, US, Jul. 2002.